THE JOURNAL OF BIOLOGICAL CHEMISTRY VOL. 285, NO. 32, pp. 25018–25023, August 6, 2010

Dopamine Induces Ca^{2+} Signaling in Astrocytes through Reactive Oxygen Species Generated by Monoamine Oxidase

Received for publication, February 5, 2010, and in revised form, June 7, 2010 Published, JBC Papers in Press, June 14, 2010, DOI 10.1074/jbc.M110.111450

Annika Vaarmann, Sonia Gandhi, and Andrey Y. Abramov[1]

From the Department of Molecular Neuroscience, UCL Institute of Neurology, Queen Square, London WC1N 3BG, United Kingdom

Dopamine is a neurotransmitter that plays a major role in a variety of brain functions, as well as in disorders such as Parkinson disease and schizophrenia. In cultured astrocytes, we have found that dopamine induces sporadic cytoplasmic calcium ($[Ca^{2+}]_c$) signals. Importantly, we show that the dopamine-induced calcium signaling is receptor-independent in midbrain, cortical, and hippocampal astrocytes. We demonstrate that the calcium signal is initiated by the metabolism of dopamine by monoamine oxidase, which produces reactive oxygen species and induces lipid peroxidation. This stimulates the activation of phospholipase C and subsequent release of calcium from the endoplasmic reticulum via the inositol 1,4,5-trisphosphate receptor mechanism. These findings have major implications on the function of astrocytes that are exposed to dopamine and may contribute to understanding the physiological role of dopamine.

Dopamine (DA)[2] is the predominant catecholamine neurotransmitter in the mammalian brain and controls a variety of functions, including locomotor activity, cognition, emotion, positive reinforcement, food intake, and endocrine regulation. The neurotransmitter DA is a monoamine that is synthesized in dopaminergic neurons in the substantia nigra in the midbrain and transferred to the striatum through very fine C-fibers (1, 2). Dopaminergic terminals constitute ~21% of total axon terminals in the striatum and contact mostly dendritic spines and dendritic shafts. The actions of DA are mediated by specific G protein-coupled receptors, which are divided into two major families based on their ability to stimulate (D1-like) or inhibit adenylate cyclase (D2-like). Three human D2-like receptors have been cloned: D2, D3, and D4 (3). Dopamergic receptors are mostly distributed in the striatum and to a lesser degree in other parts of the brain.

The signaling pathways of DA in different parts of the brain are of broad clinical and scientific interest. The neurodegenerative disorder, Parkinson disease, is caused by a loss of dopamine-secreting neurons from the midbrain; this leads to rigidity, tremor, and the characteristic slowness of movement. Impairment of DA signaling is thought to play a role not only in Parkinson disease but also Alzheimer disease and psychomotor syndromes such as schizophrenia (4–6).

[1] To whom correspondence should be addressed. E-mail: a.abramov@ucl.ac.uk.

[2] The abbreviations used are: DA, dopamine; ER, endoplasmic reticulum; HBSS, HEPES-buffered salt solution; IP_3, inositol 1,4,5-trisphosphate; MAO, monoamine oxidase; ROS, reactive oxygen species; shRNA, small hairpin RNA.

DA is catabolized by monoamine oxidase (MAO), which breaks down monoamines using FAD, producing aldehydes and hydrogen peroxide. Astrocytes express both forms of MAO: MAO-A and MAO-B (7).

Activation of D1 and D2 receptors is believed to modulate intracellular calcium levels by a single mechanism, that is, the stimulation of phosphatidylinositol hydrolysis by phospholipase C, resulting in the production of inositol 1,4,5-trisphosphate (IP_3), which mobilizes intracellular calcium stores (2, 3). Other mechanisms of release of Ca^{2+} from internal stores have also been proposed. DA increases cAMP levels (8–10). DA appears to affect the activity of calcium channels. In neurons and PC12 cells, DA reduced calcium currents by L-, N-, and P-type calcium channels (3, 9, 11). Reports on the effects of DA on intracellular calcium in astrocytes from different areas of the brain are controversial, and many of the effects cannot be explained solely by the interaction of dopamine with D1/2 receptors (3). The effect of DA on calcium homeostasis in astrocytes is potentially very important, in light of the interplay between neuronal and glial signals in physiology and pathology reported recently (12–14).

EXPERIMENTAL PROCEDURES

Cell Culture—Mixed cultures of hippocampal, cortical, or midbrain neurones and glial cells were prepared as described previously (13) with modifications, from Sprague-Dawley rat pups 2–4 days postpartum (UCL breeding colony). Hippocampi, cortex, and midbrain were removed into ice-cold HEPES-buffered salt solution (HBSS) (Ca^{2+}/Mg^{2+}-free; Invitrogen). The tissue was minced and trypsinized (0.1% for 15 min at 37 °C), triturated, and plated on poly-D-lysine-coated coverslips and cultured in Neurobasal A medium (Invitrogen) supplemented with B-27 (Invitrogen) and 2 mM L-glutamine. Cultures were maintained at 37 °C in a humidified atmosphere of 5% CO_2 and 95% air for a minimum of 12 days before experimental use to ensure the expression of receptors. Neurons were easily distinguishable from glia: they appeared phase bright, had smooth rounded somata and distinct processes, and lay just above the focal plane of the glial layer. Cells were used at 12–15 days *in vitro* unless differently stated.

Isolated cortical astrocytes were prepared as previously described (15). Cerebra taken from 2–5-day-old Sprague-Dawley rats. The cerebra were chopped and triturated until homogeneous and trypsinized (50,000 units ml^{-1} porcine pancreas; Sigma) with 336 units ml^{-1} DNase I (bovine pancreas; Sigma), and 1.033 units ml^{-1} collagenase (Sigma) at 37 °C for 15 min. After addition of fetal bovine serum (10% of final volume) and filtering through 140-μm mesh, the tissue was centrifuged

through 0.4 M sucrose (400 × *g*, 10 min), and the resulting pellet was transferred to Dulbecco's modified Eagle's medium supplemented with 5% fetal calf serum, 2 mM glutamine, and 1 mM malate in tissue culture flasks precoated with 0.01% poly-D-lysine. The cells reached confluence at 12–14 days *in vitro* and were harvested and reseeded onto 24-mm-diameter glass coverslips, precoated with 0.01% poly-D-lysine for fluorescence measurements and used for 2–4 days.

For the MAO-B knockdown experiment, cells were transiently transfected on the 2nd day *in vitro* using Lipofectamine LTX transfection reagent (Invitrogen). Empty shRNA green fluorescent protein or MAO-B containing lentiviral constructs was purchased from Open Biosystems. Cortical explant cultures were generously provided by Drs. A. V. Gourine and V. Kasymov and prepared as described in Ref. 16.

Imaging $[Ca^{2+}]_c$ and Lipid Peroxidation—For measurement of $[Ca^{2+}]_c$, primary astrocytes were loaded for 30 min at room temperature with 5 μM fura-2 AM or fluo-4 AM with/without Rhod-2 and 0.005% pluronic in a HBSS (containing 156 mM NaCl, 3 mM KCl, 2 mM $MgSO_4$, 1.25 mM KH_2PO_4, 2 mM $CaCl_2$, 10 mM glucose and 10 mM HEPES, pH adjusted to 7.35 with NaOH. Ca^{2+}-free HBSS also contained 0.5 mM EGTA. For measurement of the lipid peroxidation rate, astrocytes were loaded with 5 μM C11-BODIPY (581/591) for 30 min.

Fluorescence measurements were obtained on an epifluorescence inverted microscope equipped with a 20× fluorite objective. $[Ca^{2+}]_c$ and plasmalemmal membrane potential were monitored in single cells using excitation light provided by a xenon arc lamp, the beam passing monochromator at 340, 380, and 490 nm (Cairn Research, Kent, UK). Emitted fluorescence light was reflected through a 515-nm longpass filter to a cooled CCD camera (Retiga; QImaging) and digitized to 12-bit resolution. All imaging data were collected and analyzed using software from Andor (Belfast, UK). Traces, obtained using the cooled CCD imaging system, are presented as the ratio of excitation at 340 and 380 nm, both with emission at >515 nm. For some measurements, $[Ca^{2+}]_c$ was calculated using the equation (17) $[Ca^{2+}]_c = K(R - R_{min})/(R_{max} - R)$, where R is the fluorescence ratio (340 nm/380 nm) and K is the effective dissociation constant of fura-2. R_{max} and R_{min} were determined by application of 50 μM digitonin followed by 1 mM $MnCl_2$.

Confocal images were obtained using a Zeiss 510 UV-visible CLSM equipped with a META detection system and a 40× oil immersion objective. The 488-nm argon laser line was used to excite fluo-4, which was measured using a bandpass filter from 505–550 nm. For Rhod-2 measurements, the 543-nm laser line and 560-nm longpass filter were used. Illumination intensity was kept to a minimum (at 0.1–0.2% of laser output) to avoid phototoxicity and the pinhole set to give an optical slice of ~2 μm. C11-BODIPY (581/591) was excited using the 488- and 543-nm laser line and fluorescence measured using a bandpass filter from 505–550-nm and 560-nm longpass filter. All data presented were obtained from at least five coverslips and two or three different cell preparations. Where indicated, solvent-only control or DA-free controls were used.

Cell Viability Experiment—To measure cell viability, cells were loaded simultaneously with 20 μM propidium iodide (which is excluded from viable cells but exhibits a red fluorescence following a loss of membrane integrity in nonviable cells) and 4.5 μM Hoechst 33342 (Molecular Probes, Eugene, OR), which labels nuclei blue, to count the total number of cells. Each experiment was repeated four times using independent cultures.

Statistical Analysis—Statistical analysis was performed with the aid of Origin 8 (Microcal Software Inc., Northampton, MA) software. Means ± S.E. are expressed.

RESULTS

DA Induces a Ca^{2+} Signal in Astrocytes from Midbrain, Cortex, and Hippocampus—Application of DA (20 μM) to astrocytes in culture produced a complex fluctuation in $[Ca^{2+}]_c$ shown in Fig. 1*A*. There was no observable difference in the DA-induced Ca^{2+} signal in primary cortical, midbrain, or hippocampal astrocyte cultures, and the data shown are from experiments using cortical astrocytes, except where stated differently. To investigate the concentration of DA required to induce a Ca^{2+} signal, DA was applied in the concentration range of 0.1–100 μM to cultured astrocytes (Fig. 1*B*). Low concentrations of DA were sufficient to induce an increase in the $[Ca^{2+}]_c$, and the amplitude of the DA-induced Ca^{2+} signal (50–400 nM) was dependent on the concentration of DA applied (Fig. 1*B*).

We observed and characterized three major types of DA-induced Ca^{2+} responses in astrocytes: (i) single spikes with amplitude in the peak 200–300 nM (Fig. 1*Di*), (ii) low amplitude 150–250 nM oscillations (Fig. 1*Dii*), (iii) broad single peak of 400–500 nM (Fig. 1*Diii*). We quantified the proportion of astrocytes exhibiting each type of DA-induced Ca^{2+} signal (Fig. 1*C*). The majority of astrocytes respond to DA (20 μM) either with single spikes (46.8 ± 4.5% astrocytes) or low amplitude oscillations (40.7 ± 3.9% astrocytes). Fewer than one-fifth showed a broad single peak (12.5 ± 3.9% astrocytes) (Fig. 1*C*). After washing the cells with DA-free saline, the Ca^{2+} responses persisted for up to 5 min ($n = 38$; data not shown).

The DA-induced increase in $[Ca^{2+}]_c$ (measured by the fluo-4 fluorescence) stimulates transient Ca^{2+} uptake in mitochondria, resulting in an increase in mitochondrial $[Ca^{2+}]$ as measured by Rhod-2 fluorescence ($n = 29$; Fig. 1*E*). This mitochondrial calcium uptake is typical for physiological calcium stimuli in astrocytes.

As responses like these have not been described previously, we were concerned that the properties of cells might be dictated by our culture conditions. We therefore repeated the experiments using cortical explant cultures, in which the properties of the tissue *in vivo* are well retained. Confocal imaging of explant cultures loaded with fluo-4 demonstrated that exposure to DA (20 μM) provoked an increase in Ca^{2+} signaling in glial cells within the culture (Fig. 1*F*). (The neurons in the explants culture were identified as the only cells in the culture to show a rise in $[Ca^{2+}]_c$ with 50 mM KCl (data not shown).)

DA-induced Ca^{2+} Signal Is Receptor-independent—We sought to investigate the mechanism of the DA-induced Ca^{2+} signal. It has been shown previously that the signaling effects of DA on astrocytes are mediated by D1- and D2-like receptors (18, 19). We therefore measured the DA-induced Ca^{2+} signal in cells loaded with fura-2 in the presence and absence of DA

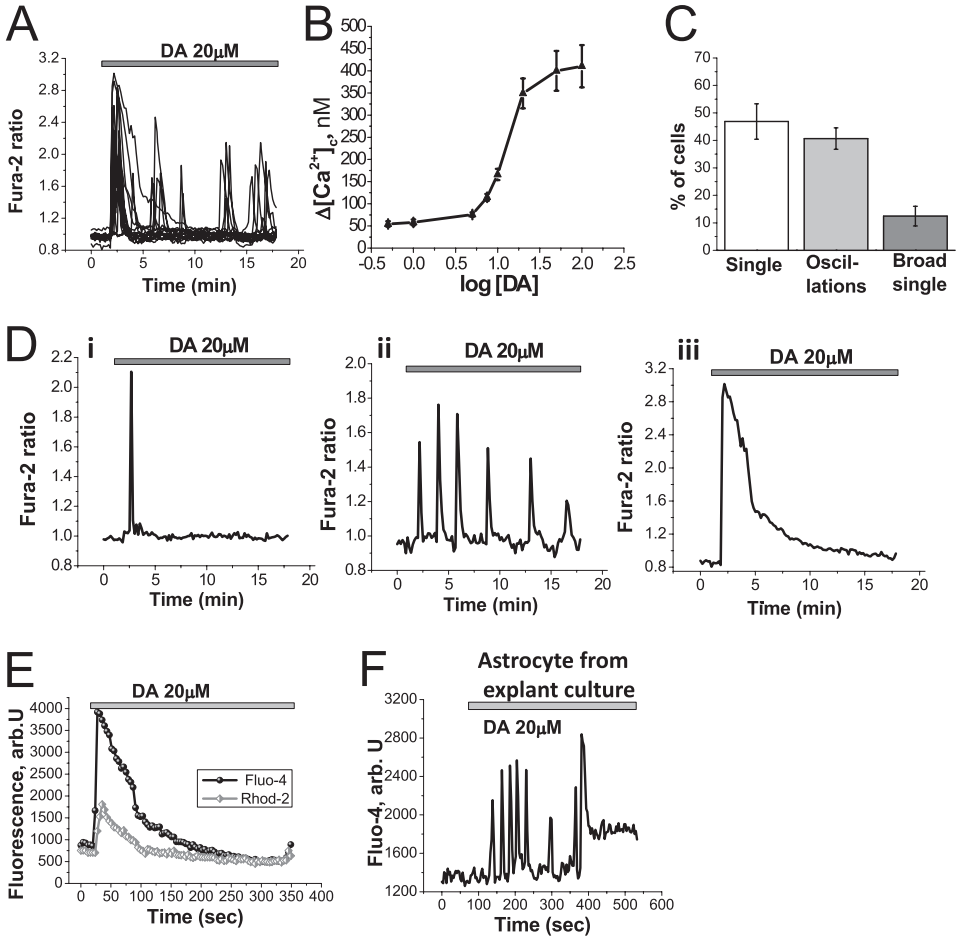

FIGURE 1. **Dopamine induces elevation of intracellular Ca^{2+} in astrocytes.** *A*, application of DA (20 μM) to astrocytes induces an immediate fluctuation in $[Ca^{2+}]_c$. *B*, amplitude of the intracellular calcium change, measured by the peak of the signal or maximal peak in the oscillations, is dependent on the concentration of DA applied. *C*, proportion of astrocytes displaying the different types of responses discussed in *D* is shown. *D*, three different types of DA-induced Ca^{2+} response were observed: single sharp spikes of Ca^{2+} flux (*Di*), sporadic increases in $[Ca^{2+}]_c$ as oscillations (*Dii*), and large increase in $[Ca^{2+}]_c$ seen as broad single peak followed by slow downward trend to baseline (*Diii*). *E*, application of DA induces a rise in $[Ca^{2+}]_c$ (measured by fluo-4; *black*) with a concomitant transient increase in $[Ca^{2+}]_m$, mitochondrial calcium (measured by Rhod-2; *gray*) in astrocytes. *F*, application of DA (20 μM) induces changes in $[Ca^{2+}]_c$, measured by fluo-4 fluorescence, in astrocytes from cortical explant culture.

receptor antagonists. Application of the antagonist for D2-like receptors (20 μM sulpiride) did not prevent the DA-induced Ca^{2+} response in astrocytes ($n = 157$; Fig. 2*A*). Similarly, application of the D1/D5 antagonist (20 μM SCH-23390) did not block the DA-induced Ca^{2+} response ($n = 171$; Fig. 2*B*). D1/D5 or D2 antagonists did not significantly change amplitude of the DA-induced Ca^{2+} signal in astrocytes. All three classes of DA-induced Ca^{2+} responses were observed in the presence of receptor antagonists. Furthermore, application of the receptor antagonists did not alter the proportion of cells exhibiting each type of DA-induced Ca^{2+} response (Fig. 2*C*). The responses to DA were also not significantly affected by inhibitors of either ionotropic or metabotropic glutamate receptors, including 10 μM MK-801 ($n = 29$ cells; Fig. 2*D*), 20 μM CNQX ($n = 34$ cells; Fig. 2*E*), or 50 μM (*S*)-MCPG ($n = 32$ cells; data not shown), suggesting that the responses do not reflect glutamate release into the culture.

We investigated the source of the Ca^{2+} in the DA-induced Ca^{2+} signal in astrocytes. Application of DA to primary cortical cell co-cultures in Ca^{2+}-free medium did not prevent the Ca^{2+} signal in astrocytes (Fig. 3*A*). This suggests that the DA-induced Ca^{2+} signal in astrocytes is dependent on intracellular Ca^{2+}. However, the absence of extracellular Ca^{2+} delayed the onset of the signal in astrocytes ($n = 80$); the time from application of dopamine to the appearance of Ca^{2+} signal was 120–180 s (Fig. 3*A*, compared with immediate onset of Ca^{2+} signal in Fig. 1*A*). Incubation of primary co-cultures with 0.5 μM thapsigargin (an inhibitor of endoplasmic reticulum (ER) Ca^{2+} pumps) depleted Ca^{2+} from the ER and completely prevented the DA-induced $[Ca^{2+}]_c$ changes in astrocytes ($n = 52$ astrocytes; Fig. 3*B*). This confirmed that the astrocytic DA-induced Ca^{2+} signal is dependent on intracellular stores.

U73122 is an inhibitor of phospholipase C. Application of U73122 completely prevented the astrocytic DA-induced Ca^{2+} signal ($n = 73$; Fig. 3*C*). Furthermore, application of 2-APB ($n = 27$ cells), an inhibitor of IP_3-dependent ER Ca^{2+} release, also blocked the DA-induced Ca^{2+} signal in astrocytes (Fig. 3*D*). Although the expression and role of ryanodine receptors in astrocytes is controversial (20), we tested the effect of the ryanodine receptor inhibitor dantrolene (10 μm), which produced no significant effect on the DA-induced Ca^{2+} signal ($n =$ 39; data not shown). Taken together, these experiments suggest that in astrocytes, DA activates phospholipase C, inducing IP_3-dependent Ca^{2+} release from ER, resulting in a rise in intracellular Ca^{2+}.

It has been reported that activation of phospholipase C and IP_3-dependent ER Ca^{2+} release can be initiated by stimulation of P_2-purinergic receptors (21). However, incubation of primary cultures of astrocytes with the P_2-purinergic receptor antagonist 20 μM PPADS (pyridoxalphosphate-6-azo(benzene-2,4-disulfonic acid) tetrasodium salt hydrate) did not affect the DA induced $[Ca^{2+}]_c$ changes in astrocytes ($n = 29$; data not shown). Therefore, DA does not activate phospholipase C via P_2-purinergic receptors.

As mentioned earlier, incubation of astrocytes in calcium-free medium (Ca^{2+}-free HBSS + 0.5 mM EGTA) induced a delay in the DA-induced Ca^{2+} signal in astrocytes. To exclude involvement of extracellular Ca^{2+} in the DA-induced Ca^{2+} signal we employed the method of manganese quench of fura-2 fluorescence. Extracellular Mn^{2+} enters cells via open

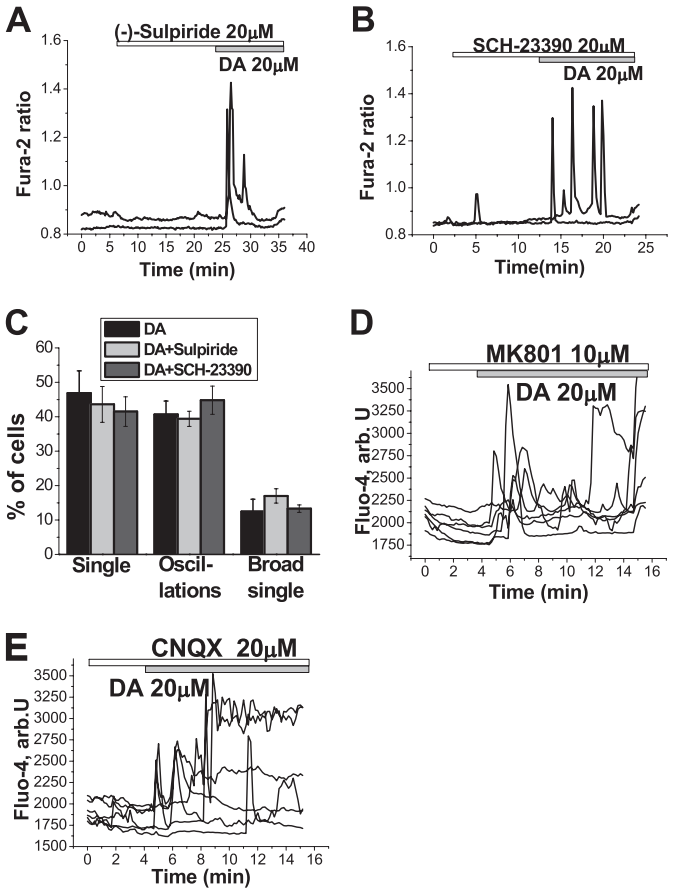

FIGURE 2. **Dopamine induces a receptor-independent $[Ca^{2+}]_c$ signal in astrocytes.** *A* and *B*, DA induces changes in $[Ca^{2+}]_c$ in astrocytes in the presence of the D2-like receptor antagonist (−)-sulpiride (20 μM (*A*) or the D1-like receptor antagonist SCH-23390 (*B*). *C*, distribution of the patterns of responses in astrocytes in response to DA in control cells and cells pretreated with (−)-sulpiride or SCH-23390 is not significantly different. *D* and *E*, inhibitors of NMDA (10 μM MK 801; *D*) or 20 μM CNQX (*E*) did not block the DA-induced Ca^{2+} signal.

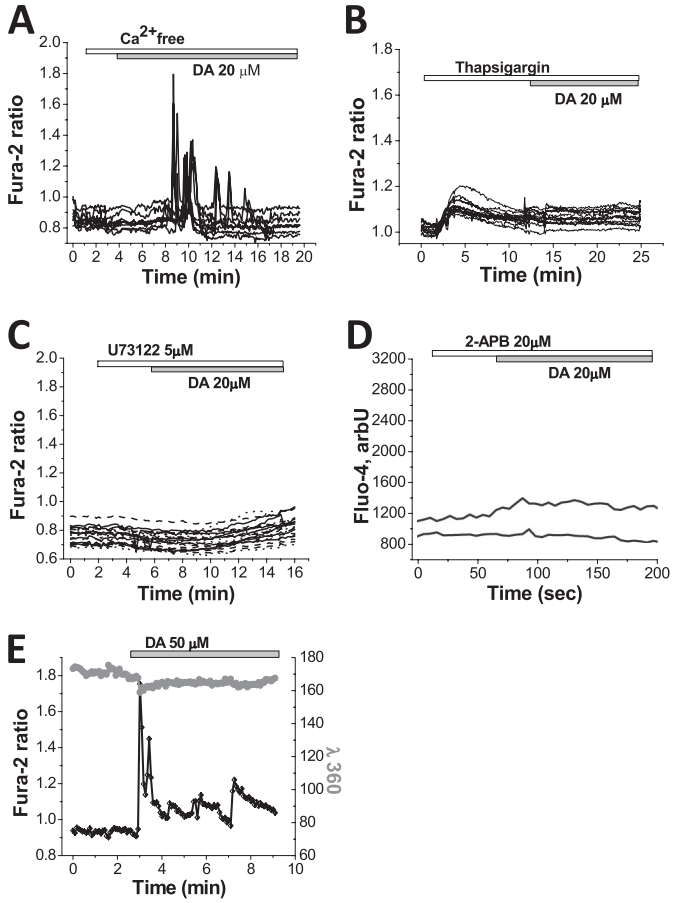

FIGURE 3. **$[Ca^{2+}]_c$ responses to dopamine are dependent on intracellular Ca^{2+} stores in astrocytes.** *A*, removal of external Ca^{2+} (Ca^{2+}-free HBSS with 0.5 mM EDTA) delays the onset of the DA-induced Ca^{2+} responses in astrocytes, but does not abolish it. *B*, depletion of the intracellular Ca^{2+} pool by application of the inhibitor of ER Ca^{2+} pump, thapsigargin (0.5 μM), abolishes the DA-induced Ca^{2+} signal in astrocytes. *C*, changes in $[Ca^{2+}]_c$ in response to DA are dependent on the presence of the inhibitor of phospholipase C U73122 (5 μM). *D*, application of the inhibitor of IP_3 receptor and capacitive calcium entrance 2-APB (20 μM) blocked the effect of DA in astrocytes. *E*, in the presence of external 100 μM Mn^{2+}, the fura-2 response excited at 360 nm showed no change during the $[Ca^{2+}]_c$ transients in astrocytes, demonstrating that this is close to the isosbestic $[Ca^{2+}]_c$-independent excitation wavelength for fura-2, confirming that the DA-induced Ca^{2+} signal in astrocytes is independent of external Ca^{2+}.

Ca^{2+}-permeate channels and quenches the fluorescence of intracellular fura-2. This is most readily seen when the fura-2 is excited at ~360 nm, the Ca^{2+}-independent (isosbestic) point of the fura-2 excitation spectrum (whereas the Ca^{2+}-dependent change of the 340/380 nm ratio is not altered by Mn^{2+}). The DA-induced Ca^{2+} spikes in astrocytes ($n = 62$) (which were recorded as high increases in the fura-2 ratio signal) induced only a small decrease in 360-nm fluorescence in the presence of Mn^{2+} (Fig. 3*E*). This experiment confirmed that extracellular Ca^{2+} does not play a role in the DA-induced $[Ca^{2+}]_c$ responses. The small changes in 360-nm signal in astrocytes (Fig. 3*E*) may be explained by the opening of store-operated Ca^{2+} channels.

DA-induced Ca^{2+} Signal in Astrocytes Is Mediated by Lipid Peroxidation—We tested the role of DA metabolism on the DA-induced Ca^{2+} signal. Monoamine oxidase is the enzyme responsible for utilization of DA in the brain (7). Preincubation (5 min) of astrocytes with the inhibitor of MAO, selegiline (20 μM inhibits both isoforms MAO-A and MAO-B) completely blocked the DA-induced Ca^{2+} signal in astrocytes ($n = 142$ astrocytes; Fig. 4*A*). Tyramine may be used as another substrate for MAO. Addition of 50 μM tyramine induced DA-like changes in the astrocyte Ca^{2+} signal ($n = 29$ cells; Fig. 4*B*), suggesting that the activity of MAO is necessary for the DA-induced Ca^{2+} signal.

To confirm the involvement of MAO in the DA-induced Ca^{2+} signal in astrocytes, we performed MAO-shRNA in midbrain co-cultures. Application of DA (20 μM) to cells with MAO knockdown did not produce a Ca^{2+} signal in astrocytes ($n = 21$; Fig. 4*C*).

MAO catalyzes DA using FAD and produces H_2O_2 and aldehyde. To test whether the Ca^{2+} signal was due to reactive oxygen species (ROS) production by MAO, we applied MnTBAP, a scavenger of ROS, to astrocytes in the presence of DA. Preincubation of primary co-cultures with 50 μM MnTBAP (a superoxide dismutase mimic and hydrogen peroxide (H_2O_2) scavenger) had no effect on the DA-induced $[Ca^{2+}]_c$ responses in astrocytes ($n = 67$ cells; Fig. 4*D*).

However, incubation of cells with an antioxidant that inhibits lipid peroxidation, 100 μM Trolox (water-soluble vitamin E analog), was effective in inhibiting the DA-induced Ca^{2+} signal

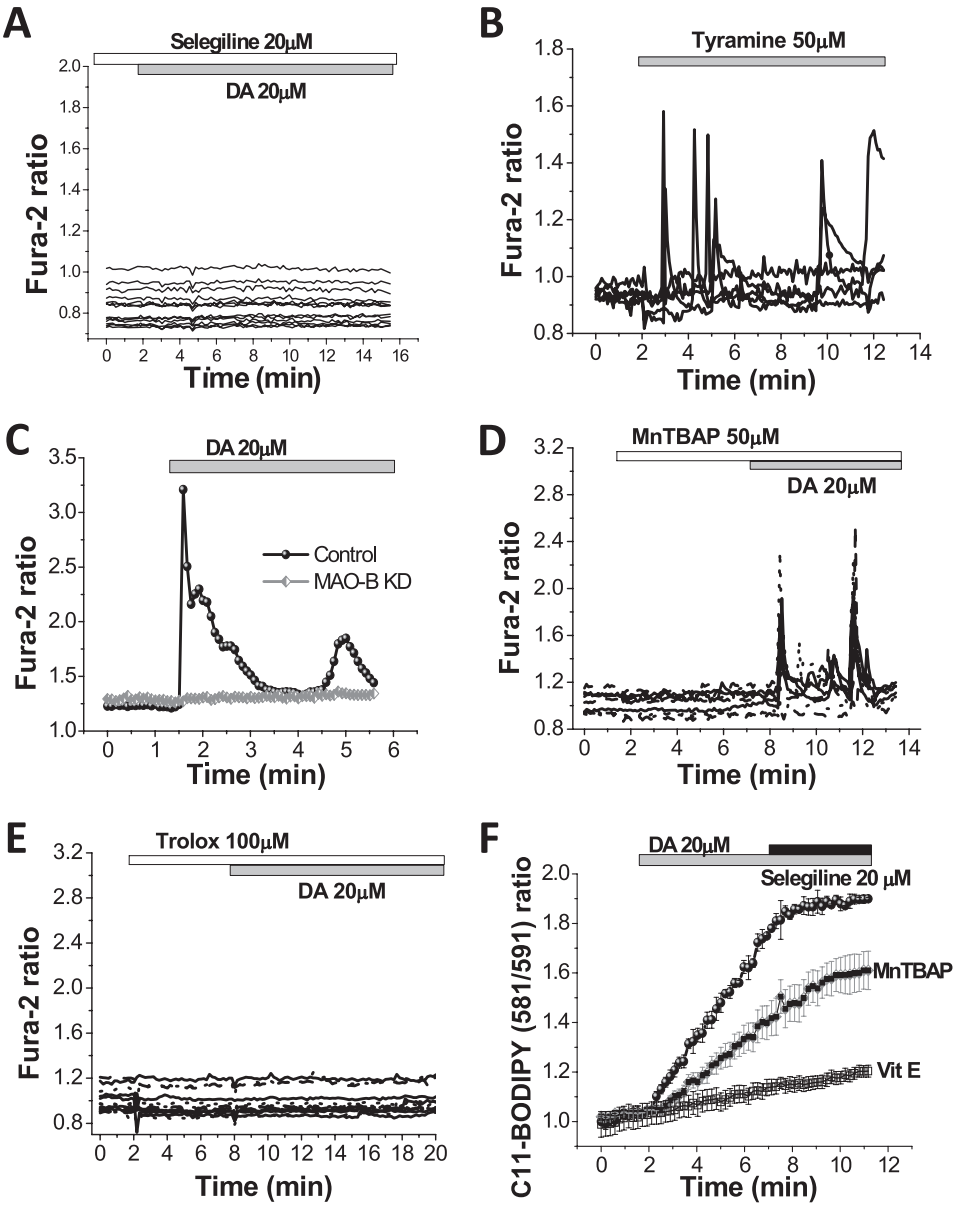

FIGURE 4. **Dopamine-induced Ca^{2+} signal in astrocytes is induced by production of ROS from MAO.** *A*, application of the MAO inhibitor, selegiline (20 μM), blocks the DA-induced Ca^{2+} signal in astrocytes. *B*, Ca^{2+} signal in primary cortical astrocytes could also induced by application of another monoamine, tyramine (50 μM). *C*, MAO-B-shRNA in astrocytes results in inhibition of the DA-induced Ca^{2+} signal. *D* and *E*, DA-induced Ca^{2+} signal was blocked by preincubation of cells with inhibitor of lipid peroxidation, Trolox (100 μM) (*D*), but not with the antioxidant MnTBAP (50 μM) (*E*). *F*, application of DA produces a rise in the rate of lipid peroxidation in astrocytes, which is dependent on MAO activity. DA-induced lipid peroxidation could be prevented by pretreatment of astrocytes with α-tocopherol (100 μM). Pretreatment of astrocytes with the antioxidant MnTBAP (50 μM) reduced the rate of lipid peroxidation but did not abolish it.

in astrocytes ($n = 81$ cells; Fig. 4*E*). It should be noted that Trolox is a water-soluble antioxidant and can be effective at ROS scavenging in the cytosol. 50-min preincubation of the cells with 100 μM vitamin E (α-tocopherol) also completely prevented the DA-induced Ca^{2+} signal in astrocytes ($n = 49$; data not shown).

To test whether DA affects lipid peroxidation, we employed the specific indicator C11-BODIPY (581/591), which allows live changes in the rate of lipid peroxidation in live cells to be measured. Addition of 20 μM DA induced a rapid increase in the rate of lipid peroxidation in astrocytes (signal rose to 315.3 ± 26% of basal rate, $p < 0.001$; $n = 36$ cells; Fig. 4*F*). The effect of DA on lipid peroxidation was induced by the activation of MAO as it could be blocked by application of the MAO inhibitor selegiline 20 μM (rate of C11-BODIPY (581/591) oxidation dropped from 315.3 ± 26% to 95.3 ± 6.2% of basal rate; Fig. 4*F*). Considering the differences in the effect of MnTBAP and vitamin E on DA-induced Ca^{2+} signaling, we also tested the effect of these two antioxidants on DA-stimulated lipid peroxidation. Pretreatment of astrocytes with α-tocopherol (100 μM, 20 min) completely prevented the increase in the rate of DA-induced lipid peroxidation (108.6 ± 6.8% of basal rate C11-BODIPY (581/591) oxidation, $n = 27$; Fig. 4*F*). Exposure of astrocytes with 50 μM MnTBAP (20 min before and during the time of experiment) did not abolish DA-induced lipid peroxidation but did result in a reduction in the rate of peroxidation. The rate of C11-BODIPY (581/591) oxidation in cells treated with MnTBAP rose to 231.4 ± 28.3% in response to DA ($n = 34$; $p < 0.001$; Fig. 4*F*). Thus, MnTBAP is not as effective against DA-induced lipid peroxidation as α-tocopherol, and this may underlie the difference in the of vitamin E and MnTBAP on the DA-induced Ca^{2+} signal. Thus, activation of MAO in astrocytes by DA induces lipid peroxidation which leads to the stimulation of phospholipase C and IP_3-induced calcium release from ER.

DA-induced Ca^{2+} Signaling Occurs at DA Concentrations That Do Not Affect Cell Viability—The *in vivo* concentration of DA is not well established, and different authors report physiological ranges of DA concentration in the nanomolar to millimolar range. To establish whether the concentration of DA that induces a Ca^{2+} signal in astrocytes is pathological, we studied the effect of different concentrations of DA (0–500 μM) on the viability of astrocytes. Prolonged (24-h) exposure of 5–50 μM DA did not significantly increase the number of cell death in primary cultures of cortical astrocytes (Fig. 5) compared with control. Only high concentrations of DA (100 μM and 500 μM) produced a significant increase in cell death (from 14.3 ± 2.9% in control to 27.8 ± 3.9% for 100 μM of DA; $p < 0.01$; and to 73.6 ± 5.5% for 500 μM; $p < 0.001$; $n = 3$, Fig. 5). Thus, the changes in $[Ca^{2+}]_c$ in astrocytes in response to

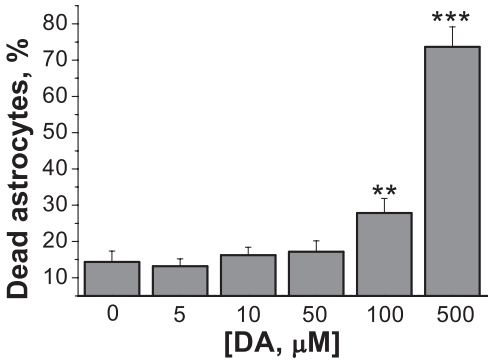

FIGURE 5. **Effect of DA on cell viability.** Low concentrations of DA (0–50 μM) have no significant effect on cell viability in pure cultures of cortical astrocytes, whereas higher concentrations (100, 500 μM) significantly increased the percentage of cell death. **, $p < 0.01$; ***, $p < 0.001$ *versus* control. All data are expressed as mean ± S.E. (*error bars*).

the concentrations of DA used in these experiments are not reflected in pathological processes in cells.

DISCUSSION

Our findings suggest novel effects of DA on calcium signaling in astrocytes. Astrocytes and neurons are likely to communicate both physiologically and in disease. Physiologically, calcium signals in astrocytes cause cerebrovascular constrictions (22, 23). Neurotoxicity in neurodegenerative disease may be mediated by astrocyte-neuronal interactions. For example, β-amyloid induces a calcium signal in astrocytes which results in overproduction of ROS, reduction of antioxidant levels, and cell death in neurons (12–14). In this study, we have demonstrated that metabolism of nontoxic concentrations of DA by MAO in astrocytes produces hydrogen peroxide, which activates lipid peroxidation in the neighboring membranes. Lipid peroxidation activates phospholipase C, releasing IP_3 and inducing a Ca^{2+} signal. Although ROS have been extensively implicated in causing oxidative damage in neurodegenerative disease, there is emerging evidence that ROS also acts as a physiological mediator of normal cellular function. The cellular redox state and ROS may stimulate as well as inhibit Ca^{2+} channels and Ca^{2+} pumps and thus modulate Ca^{2+} signaling (24). To our knowledge this is a first evidence of the involvement of ROS in a calcium signaling pathway in response to a physiological stimulus such as dopamine transmission in the brain.

Increased levels of oxidative stress in the brain may be critical for the initiation of glutamate or ATP release, which acts as a trigger for Ca^{2+} signaling (25–27). In skeletal and cardiac muscle, ROS is known to induce a calcium signal via activation of the ryanodine receptor (28). However, we have shown that this mechanism is not involved in DA-induced $[Ca^{2+}]_c$ changes because the astrocytic calcium signal was insensitive to inhibitors of glutamate, purinergic, or ryanadine receptors (see above). DA can produce ROS via both enzymatic (H_2O_2) and nonenzymatic metabolism (H_2O_2, superoxide) (29). However, the effect of the MAO inhibitor selegiline and the effect of MAO-shRNA confirmed the role of enzymatic ROS production on lipid peroxidation and the induction of calcium signaling in astrocytes.

We have shown for the first time that DA produces effects on Ca^{2+} signaling that are not mediated by the known receptors. Of note, this is the first demonstration of Ca^{2+} signaling in astrocytes mediated by ROS. We believe that this DA-induced Ca^{2+} signal may play an important role in dopamine signaling in human brain.

Acknowledgments—We thank Parkinson UK for support and Dr. Vitaliy Kasimov and Dr. Alexander V. Gourine for providing cortical explant cultures. We are also grateful to Victoria Burchell for assistance.

REFERENCES

1. Dahlström, A., and Fuxe, K. (1964) *Experientia* **20,** 398–399
2. Kötter, R. (1994) *Prog. Neurobiol.* **44,** 163–196
3. Missale, C., Nash, S. R., Robinson, S. W., Jaber, M., and Caron, M. G. (1998) *Physiol. Rev.* **78,** 189–225
4. Nemeroff, C. B., and Bissette, G. (1988) *Ann. N.Y. Acad. Sci.* **537,** 273–291
5. Sulzer, D., and Schmitz, Y. (2007) *Neuron* **55,** 8–10
6. Surmeier, D. J. (2007) *Lancet Neurol.* **6,** 933–938
7. Youdim, M. B., and Bakhle, Y. S. (2006) *Br. J. Pharmacol.* **147,** Suppl. 1, S287–S296
8. Lin, C. W., Miller, T. R., Witte, D. G., Bianchi, B. R., Stashko, M., Manelli, A. M., and Frail, D. E. (1995) *Mol. Pharmacol.* **47,** 131–139
9. Cantuti-Castelvetri, I., and Joseph, J. A. (1999) *Free Radic. Biol. Med.* **27,** 1393–1404
10. Tang, T. S., and Bezprozvanny, I. (2004) *J. Biol. Chem.* **279,** 42082–42094
11. Surmeier, D. J., Bargas, J., Hemmings, H. C., Jr., Nairn, A. C., and Greengard, P. (1995) *Neuron* **14,** 385–397
12. Haydon, P. G. (2001) *Nat. Rev. Neurosci.* **2,** 185–193
13. Abramov, A. Y., Canevari, L., and Duchen, M. R. (2003) *J. Neurosci.* **23,** 5088–5095
14. Abramov, A. Y., Canevari, L., and Duchen, M. R. (2004) *Biochim. Biophys. Acta* **1742,** 81–87
15. Pavlov, E., Aschar-Sobbi, R., Campanella, M., Turner, R. J., Gómez-García, M. R., and Abramov, A. Y. (2010) *J. Biol. Chem.* **285,** 9420–9428
16. Teschemacher, A. G., Paton, J. F., and Kasparov, S. (2005) *Adv. Drug Deliv. Rev.* **57,** 79–93
17. Grynkiewicz, G., Poenie, M., and Tsien, R. Y. (1985) *J. Biol. Chem.* **260,** 3440–3450
18. Liu, J., Wang, F., Huang, C., Long, L. H., Wu, W. N., Cai, F., Wang, J. H., Ma, L. Q., and Chen, J. G. (2009) *Cell. Mol. Neurobiol.* **29,** 317–328
19. Zhang, X., Zhou, Z., Wang, D., Li, A., Yin, Y., Gu, X., Ding, F., Zhen, X., and Zhou, J. (2009) *J. Neurosci.* **29,** 7766–7775
20. Matyash, M., Matyash, V., Nolte, C., Sorrentino, V., and Kettenmann, H. (2002) *FASEB J.* **16,** 84–86
21. Peuchen, S., Clark, J. B., and Duchen, M. R. (1996) *Neuroscience* **71,** 871–883
22. Mulligan, S. J., and MacVicar, B. A. (2004) *Nature* **431,** 195–199
23. Gordon, G. R., Choi, H. B., Rungta, R. L., Ellis-Davies, G. C., and MacVicar, B. A. (2008) *Nature* **456,** 745–749
24. Feissner, R. F., Skalska, J., Gaum, W. E., and Sheu, S. S. (2009) *Front. Biosci.* **14,** 1197–1218
25. Avshalumov, M. V., and Rice, M. E. (2003) *Proc. Natl. Acad. Sci. U.S.A.* **100,** 11729–11734
26. Gonzalez-Islas, C., and Hablitz, J. J. (2003) *J. Neurosci.* **23,** 867–875
27. González, A., Granados, M. P., Pariente, J. A., and Salido, G. M. (2006) *Neurochem. Res.* **31,** 741–750
28. Hidalgo, C., Bull, R., Marengo, J. J., Perez, C. F., and Donoso, P. (2000) *Biol. Res.* **33,** 113–124
29. Chinta, S. J., and Andersen, J. K. (2008) *Biochim. Biophys. Acta* **1780,** 1362–1367